

TECHNOTE



U.S. Department of Transportation
Federal Highway Administration

Turner-Fairbank
Highway Research Center

Research, Development,
and Technology
Turner-Fairbank Highway
Research Center
6300 Georgetown Pike
McLean, VA 22101-2296

<https://highways.dot.gov/research>

Pocket Lidar Culvert Assessments

FHWA Publication No.: FHWA-HRT-25-016

FHWA Contact: Matthew Corrigan
(ORCID: 0000-0002-1230-8462), Federal Highway
Administration (FHWA) Infrastructure Analysis and
Construction Team (HRDI-20), 202-493-3365,
matthew.corrigan@dot.gov

This document is a technical summary of a case study for the FHWA report *Leveraging Pocket Lidar for Construction Inspection and Digital As-Builts—Phase 1 (Forthcoming)*.

OVERVIEW

Culverts serve as important infrastructure, allowing water from streams, rivers, and engineered drainage systems to pass underneath roadways to prevent flooding and erosion. Culverts can be designed in a wide range of configurations and shapes, including pipe arch, box, circular, and elliptical culverts.⁽¹⁾ In addition to verification of design compliance at construction, culverts require routine assessment and maintenance to ensure proper operation. Verifying proper construction or assessing culvert conditions can be challenging given the need to acquire measurements in images in tight spaces with low light, flowing water, debris, difficult access, etc. Many survey and imaging devices are not feasible to operate in such situations.

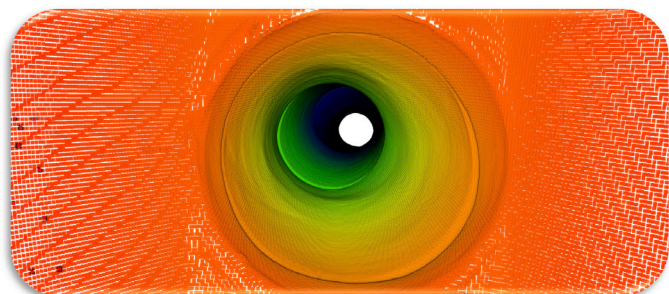
Pocket lidar's (PL) small size and portability make PL a promising tool to aid inspectors in acquiring measurement and other condition information during the assessment process. This case study had the following objectives:

- Determine the feasibility of acquiring measurements and imagery in culverts to support assessments.
- Evaluate the accuracy of the data compared to a survey-grade lidar system obtaining key dimensions of the culvert.
- Evaluate the influence of lighting sources on the resulting data products.
- Evaluate the ability to capture obstructions due to debris in the culvert.

This case study explores the use of PL for culvert inspections (figure 1). This project was carried out in collaboration with the Utah Local Technology Assistance Program (LTAP) and the Utah Department of Transportation (UDOT). This case study supported an extensive research project underway by Utah LTAP evaluating a variety of technologies to obtain metrics for culvert damage assessments.

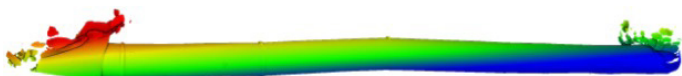
In conjunction with the data-collection efforts, the research team gave a presentation summarizing key results of the overall FHWA project exploring PL and performed technology demonstrations at the Midas Creek culvert site where participants could obtain hands-on experience operating PL.

Figure 1. Screenshots. Example point cloud of a culvert showing deformation.



Source: FHWA. Created using data from Leica RTC360 visualized in CloudCompare version 2.13.⁽²⁾

A. View looking into the culvert.



Source: FHWA. Created using data from 3D Scanner App visualized in CloudCompare version 2.13.^(2,3)

B. View looking at the culvert elevation profile.

DATA COLLECTION AND FIELD SITES

Several months before conducting the field surveys, Utah LTAP identified candidate culverts in relatively close proximity to economize travel time while still capturing different pipe conditions (e.g., debris and damage levels), materials, and sizes. For feasibility, only culverts 48 inches or larger in diameter were considered. Smaller culverts could potentially be acquired with a robotic platform or rolling platform; however, that equipment was beyond the scope of this pilot study (performing an initial assessment of the capabilities and limitations of PL for culvert assessment). Table 1 summarizes the culverts captured in the field effort.

The research team captured data for a total of 11 culverts over the course of 1.5 d in August 2023 when peak flows from snowmelt had subsided to ensure safe operation. Due to abnormally high levels of snowfall in Utah in the 2022–2023 winter season, high flow rates continued much later into the summer than usual. The team used an Apple® iPhone™ 13 Pro Max and iPhone 14 Pro to collect the data using the Laan Labs® 3D Scanner App and Niantic, Inc. Scaniverse.^(3,4)

(The specific phone and app used varied for each site.) The lidar sensor specifications are the same between the iPhone 13 Pro Max and iPhone 14 Pro. Each pass with PL generally took 2–5 min to complete but varied based on the length of the pipe and the difficulty of moving through the pipe. Reference data were collected using the Leica® RTC360 laser scanner generally set to high resolution (3.1-mm sampling at 10-m range) for the larger pipes and medium resolution (6.3-mm sampling at 10-m range) for the smaller pipes.

DATA PROCESSING

The research team registered RTC360 static scanner reference data in Leica Cyclone software and cropped to the extent of the culvert.⁽⁶⁾ For workability, the scans were then exported and subsampled to 0.005 m or 0.01 m (depending on the size of the pipe) using a voxelization procedure in the EZDataMD EZVox software.⁽⁷⁾ This process organizes the point clouds into voxels (three-dimensional (3D) cells) at the desired spacing and then keeps only the point closest to the center of each voxel. This approach helps maintain a more uniform point distribution and preserves key shapes and features in the dataset by not smoothing the data.⁽⁸⁾

The PL data exported from the apps were postprocessed in CloudCompare software.⁽⁹⁾ First, the team registered the PL scan to the same local coordinate system as the RTC360 reference scans through an iterative closest point (ICP) alignment procedure.⁽¹⁰⁾ Leveling was constrained for the registration so that PL kept the sensor-based leveling instead of adjusting to the RTC360 data to ensure that PL's leveling quality and ability to capture slope gradient information could be evaluated. Only PL's position in X, Y, Z, and bearing (rotation Z) were allowed to adjust in the registration. Multiple iterations were repeated until the solution was stable and converged.

The research team completed several additional analyses for selected culverts, such as extracting cross sections to obtain measurements of width, height, length, and area. The EZDataMD EZFitter tool was used to fit circles and ellipses to the extracted cross sections from CloudCompare to obtain pipe diameters and evaluate PL's ability to capture the shape of the pipe.^(8,9,11) For cross-sectional area computations, two-dimensional (2D) polygon facet fitting was performed in CloudCompare software. The team used spreadsheet software to perform computations of slope from extracted profiles and coordinates.

Table 1. Summary of sites captured with PL.

ID	Short Code	Site Name	Location (Utah)	Type	Nominal Diameter (inch/m)	Length (m)	PL App	RTC	Comments
1	MC	Midas Creek	Herriman: Anthem Boulevard and Bigbend Park Drive	CM, elliptical	380/9.65 (major axis)	32.0	3D Scanner App, ⁽³⁾ Scaniverse, ⁽⁴⁾ Metascan, ⁽⁵⁾ Pix4D ⁽⁶⁾	Y	Elliptical metal pipe arch over Midas Creek and Trail. Could not capture the full culvert with PL from path. Could almost capture the full culvert from the rocks in the creek bed; however, the full culvert was difficult to scan while walking on the rocks. Closed loop scans with RTC360.
2	MR	Miller Crossing	Herriman: Miller Crossing Lane and Ryeland Drive	RCP	72/1.83	—	3D Scanner App ⁽³⁾	Y	Recently constructed pipe with smooth walls, minimal signs of distress. Pipe continues for a long distance. Only 115 m of pipe at the outlet was scanned. Pipe has a maintenance hole opening and a substantial curve in pipe. Scans were captured with different supplemental lights. Could not directly close loop with RTC360.
3	LF	Lisa Falls	Little Cottonwood Canyon	Polypropylene triple wall	60/1.52	27.7	Scaniverse ⁽⁴⁾	Y	Relatively new pipe showing signs of distress as well as large shifts. Full pipe scanned with RTC360 (closed loop) and PL.
4	TP	Tanner Park Little	Salt Lake City: Tanner Park	CM	48/1.22	9.0	3D Scanner App, ⁽³⁾ Scaniverse ⁽⁴⁾	Y	Full pipe scanned with RTC360 (closed loop) and PL. Substantial damage to and debris present in pipe.
5	ST	Shoot The Tube	I-80, Tanner Park	RCP	92/2.34	—	3D Scanner App, ⁽³⁾ Scaniverse ⁽⁴⁾	N	Pipe was too long and flows were too high to capture the entire pipe with PL. Captured some data for a short section at the outlet. No RTC360 scans were collected.
6	CC	Country Club	I-80, Tanner Park	RCP	92/2.34	—	Scaniverse ⁽⁴⁾	N	Small portion of pipe was scanned with PL. No RTC360 scans were collected.

Table 1. Summary of sites captured with PL. (Continued)

ID	Short Code	Site Name	Location (Utah)	Type	Nominal Diameter (inch/m)	Length (m)	PL App	RTC	Comments
7	BB	Parley's Canyon Big Box	I-80	RCP	66/1.68	—	Scaniverse ⁽⁴⁾	N	Flows still too high to access interior. Captured pipe outlet and box with PL. Could extract the diameter of the pipe. No RTC360 scans were collected.
8	I80-2	I-80 MP132	I-80, MP132 Westbound	CM	96/2.44	—	3D Scanner App, ⁽³⁾ Scaniverse ⁽⁴⁾	N	Access to the pipe is difficult. A portion of the pipe was scanned with PL but was not feasible for a static scanner.
9	I80-1	I-80 MP131.4	I-80, MP131.4 Westbound	CM	82/2.08	—	3D Scanner App, ⁽³⁾ Scaniverse ⁽⁴⁾	N	Access to the pipe is difficult. A portion of the pipe was scanned with PL but was not feasible for a static scanner.
10	HG	Hidden Grove	Salt Lake City: Sugar House Park, Hidden Grove Basketball Court	CM	98/2.49	94.0	Scaniverse ⁽⁴⁾	Y	Still, substantial water was present in the pipe but at a very low flow rate. The full pipe was scanned with both PL and the RTC360. Could not close the loop with RTC360. The first 4.5 m could not be safely captured with PL at the outlet because overhanging pipe was damaged at the bottom.
11	PCP	Parley's Creek Pavilion	Salt Lake City: Sugar House Park, Parley's Creek Pavilion	RCP	60/1.52	19.0	3D Scanner App, ⁽³⁾ Scaniverse ⁽⁴⁾	Y	A hydraulic jump was present in the pipe. Flows were too fast and water levels too high to perform RTC360 scans inside of the pipe. However, the RTC360 was still able to capture most of the pipe, albeit from oblique angles. Closed loop with RTC scans. Clogging of the catch basin. The full pipe was scanned with PL.

—No data.

ID = identification number; RTC = Leica® RTC360 laser scanner; CM = corrugated metal; RCP = reinforced concrete pipe.

EXAMPLE ANALYSES

Herriman Midas Creek

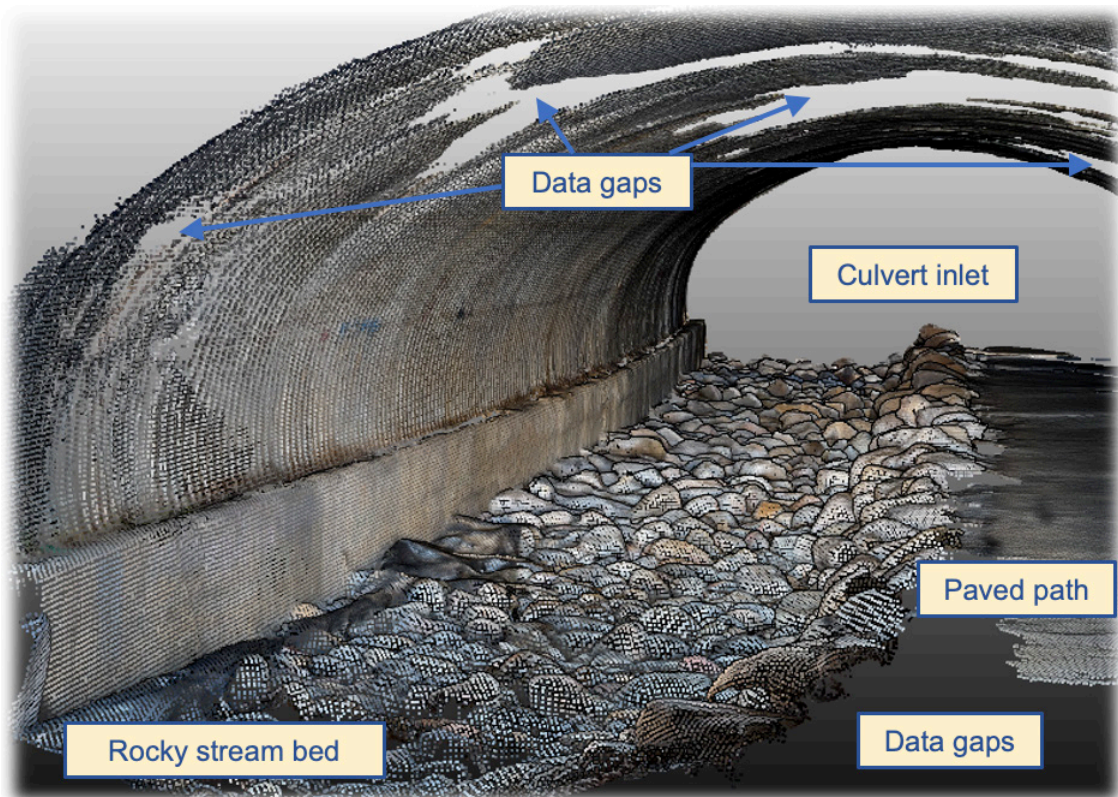
The demonstration was at Midas Creek because access was easy for participants. Data collection with PL in the Midas Creek culvert used three apps: Abound Labs Inc. Metascan; Niantic, Inc. Scaniverse; and Laan Labs 3D Scanner App.^(2,3,4) The team also obtained reference data with the RTC360. A total of 15 scans were collected as a closed loop passing both through the culvert and across the road above the culvert to minimize any drift within the RTC360 data.⁽¹²⁾ Both Scaniverse and 3D Scanner App struggled to capture the entire culvert in a single pass due to the culvert's large size and the range limitations of PL (5 m in ideal conditions) (figure 2). Multiple passes were performed with adjustments to settings to attempt to improve the data capture. Metascan was able to provide a full scan of the culvert in a single pass; however, the resulting point cloud had many reconstruction artifacts because the app relied solely on photogrammetric solutions to overcome the range limitations of the lidar sensor. Additionally, substantial smoothing of surfaces was observed in the Metascan models.⁽⁵⁾

Herriman: Miller's Crossing

The team scanned only a 115-m section of the Miller's Crossing culvert at the outlet due to the extensive length of the pipe. At this section, the pipe contained a substantial direction change at a maintenance access hole. Several light sources (figure 3) were tested at this site to determine the effect of lighting on the reconstruction quality, including the following light sources:

1. A small headlamp.
2. A small handheld light with two lights with some ability to adjust along a single axis (1,000-lumen light-emitting diode (LED) work light).
3. A larger handheld light with three lights that could be adjusted in a variety of directions (2,000-lumen LED rechargeable work light and detachable spotlight).
4. A small 500-lumen LED light source that could be attached directly to the iPhone .
5. A combination of lights 1, 3, and 4.

Figure 2. Illustration. Example scan of Mires Creek: PL struggled to capture the entire culvert due to the size of the culvert, resulting in substantial data gaps.



Source: FHWA. Created using data from Metascan visualized in CloudCompare version 2.13.^(2,5)

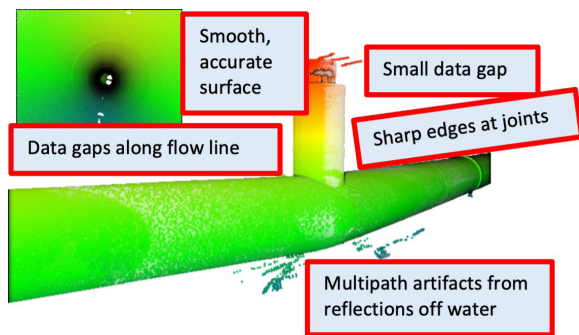
Figure 3. Photo. Example data collection with three different lighting sources.



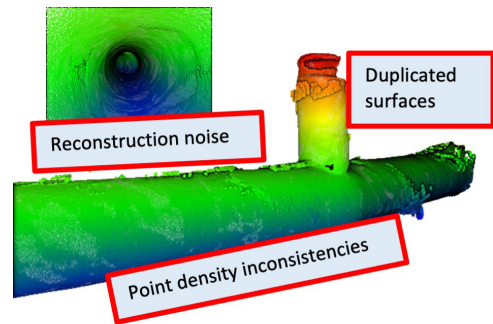
Source: FHWA.

The lighting source substantially affected PL 3D reconstruction quality. Figure 4 shows examples of data collected with each light source. The headlamp (1) provided insufficient lighting and resulted in very poor reconstruction with many duplicative surfaces. The double light source improved results but still had substantial noise. The reconstruction was of much higher quality with the three-directional light source. The reconstruction was generally good when using the attachment light. However, despite the use of strong hook and loop fasteners, the light was difficult to keep firmly attached to PL as the operator moved PL around during the data collection process. When using light sources 1, 3, and 4 in combination, the data contained several areas of artifacts, so a lighting source similar to the three-directional light is recommended for better results. This light was then used as the primary light source on other culverts.

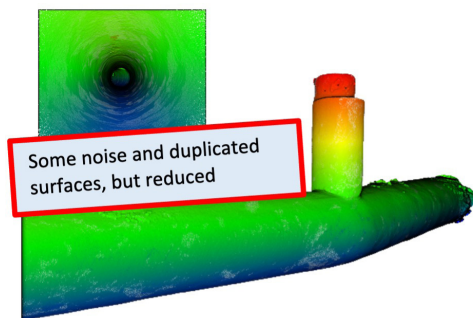
Figure 4. Illustration. Comparison of point clouds obtained with different lighting sources for the Miller's Crossing culvert.



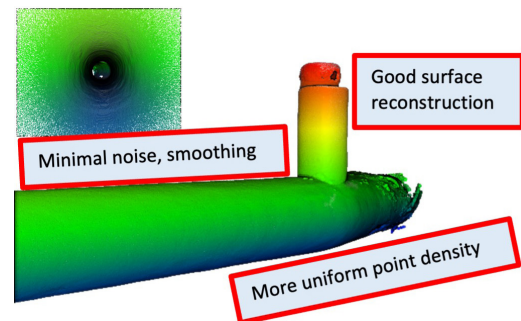
A. RTC360 reference scan.



B. PL with headlamp.



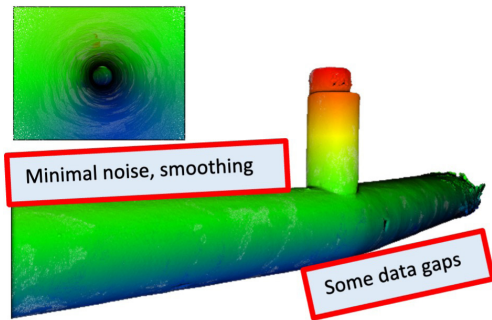
C. PL with double light source.



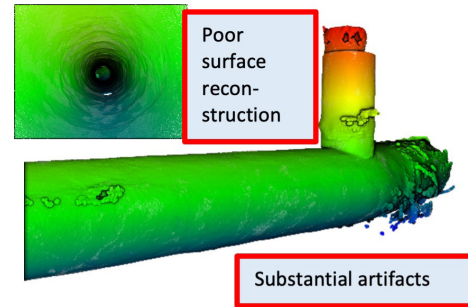
D. PL with three directional lights.

Source: FHWA. Created using RTC360 and 3D Scanner App visualized in CloudCompare version 2.13.^(2,3)

Figure 4. Illustration. Comparison of point clouds obtained with different lighting sources for the Miller's Crossing culvert. (Continued)



E. PL with attached light.



F. PL with combination of b, d, and e.

Source: FHWA. Created using RTC360 and 3D Scanner App visualized in CloudCompare version 2.13.^(2,3)

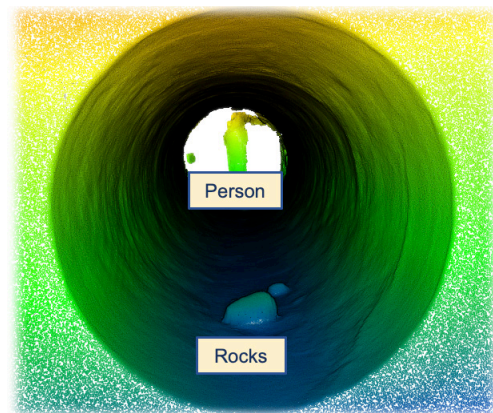
Note that all PL scans had substantial artifacts for an approximately 2-m section at the start of the data-collection section in the culvert, likely due to difficulty initializing in the dark in an underground space. When scanning is completed for just a portion of the pipe, scanning at least a few meters beyond the area of interest at the start and end points of the pipe is recommended. Then the operator can use the apps to crop the data and remove the artifacts without affecting the area of interest.

Small rocks near the outlet of the culvert were clearly distinguishable in the PL data (figure 5). Small cracks and spalling were visible near a joint in the culvert; however, those cracks and spalling could not be distinguished in the point cloud data from PL. While these cracks and spalling were captured in the texture-mapped mesh (figure 6), they were somewhat difficult to distinguish in the mesh from photogrammetric stitching artifacts and prolific graffiti in the culvert. However, the joint and spalling could not be detected from mesh geometry itself.

Lisa Falls

The culvert at Lisa Falls is a relatively new 48-inch diameter polypropylene (triple wall) pipe in Little Cottonwood Canyon that has experienced some distortion, resulting in a bend in the pipe three-quarters of the length of the pipe in from the pipe's inlet (figure 7a). The data analysis focuses on PL's ability to capture the general shape of the culvert as well as the distortion. Small bumps were observed at the bottom of the pipe, indicating distress. The pipe length was measured at 27.718 m with PL compared with 27.692 m from the RTC360, resulting in a small difference of +0.027 m or +0.09 percent.

Figure 5. Illustration. Examples of rock debris near the outlet of the culvert.



Source: FHWA. Created using data from 3D Scanner App visualized in CloudCompare version 2.13.^(2,3)

Figure 6. Screenshot. Closeup of spalling at a joint in the culvert in the texture-mapped mesh.



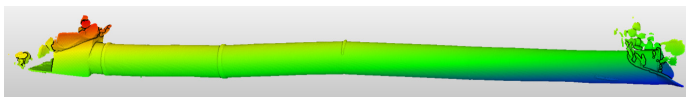
Source: FHWA. Created using data from 3D Scanner App visualized in CloudCompare version 2.13.^(2,3)

The research team took a total of 25 0.05-m wide vertical cross sections (figure 7b) at coincident locations in both PL and RTC360 point clouds. A circle was then fitted using orthogonal least squares regression to the point cloud data in the best fit plane of each cross section using the EZDataMD EZFitter tool.⁽¹¹⁾ The team computed several metrics (table 2) to evaluate the data quality, including the following metrics:

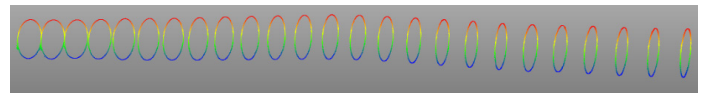
- The root mean square (RMS) deviations described the quality of the fit of the points to the circle. Overall, the fit quality was similar between PL and the RTC360. The cross sections with a few centimeters RMS were at the portion of the pipe at the exterior where data were obtained on both the inside and outside of the pipe.

- The radius of the pipe was compared between the PL and RTC360 for each cross section. Overall, the radii were very similar—within 0.005 m RMS.
- Circle center position in X, Y, and Z captured the drift of PL as a longer area was captured. Decimeter-level drift in the X and Y directions were observed; however, less drift was observed vertically.
- Slope gradient could be used to evaluate the leveling quality of the scanner and the scanner’s ability to capture the pipe’s flow line for hydraulic modeling and capacity analysis. The slope gradient was computed based on the elevation changes and horizontal distances between the lowest points of each adjacent fitted circle to represent the pipe flowline. The differences in slope gradients were within 0.43 percent RMS.

Figure 7. Illustrations. Side view of the Lisa Falls culvert.



A. Full point cloud for the culvert.



B. Extracted cross sections of the culvert.

Source: FHWA. Created using data from 3D Scanner App visualized in CloudCompare version 2.13.^(2,3)

Table 2. Circular fitting results of PL compared with the RTC360 reference scans at Lisa Falls.

Statistic	RMS (PL)	RMS (RTC360)	Δ RMS	Δ Radius	Δ X center	Δ Y center	Δ Z center	Δ Slope (percent)
Average (m)	0.0098	0.0096	0.0002	-0.0048	-0.0209	0.0441	-0.0044	-0.12
Std. dev. (m)	0.0099	0.0097	0.0013	0.0020	0.0217	0.0462	0.0159	0.42
Minimum (m)	0.0018	0.0014	-0.0019	-0.0078	-0.0649	-0.0068	-0.0268	-0.74
Maximum (m)	0.0342	0.0354	0.0035	0.0002	0.0042	0.1380	0.0177	0.79
RMS (m)	0.0138	0.0135	0.0013	0.0052	0.0298	0.0631	0.0162	0.43
95% conf. (m)	0.0270	0.0265	0.0025	0.0101	0.0584	0.1237	0.0317	0.84
Count	25	25	25	25	25	25	25	24

Std. dev. = standard deviation; conf. = confidence interval; Δ = delta.

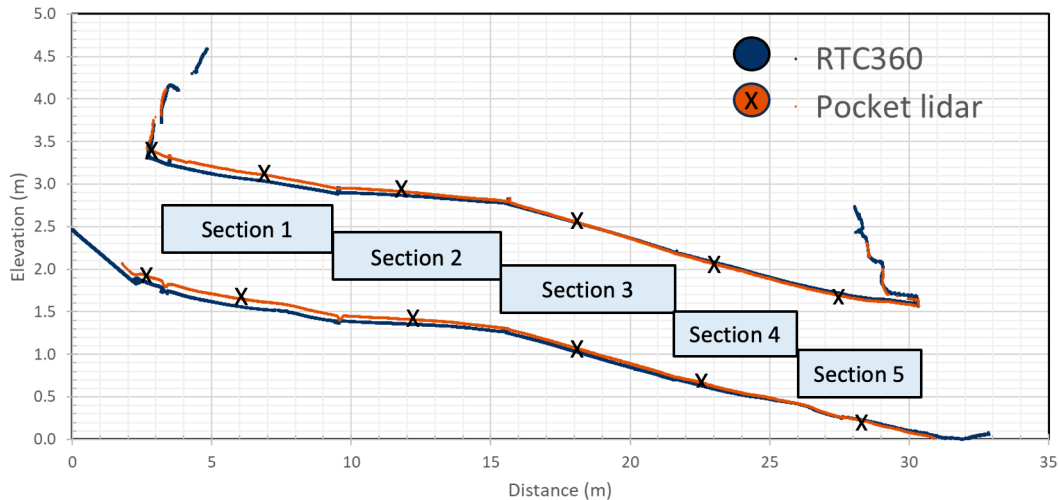
Following the analysis of the transverse cross sections, a longitudinal cross section was extracted from the PL and RTC360 reference data along the flowline of the pipe. The pipe was divided into five sections based on the locations of joints within the pipe (figure 8). The research team computed slopes using the following two methods:

- Method 1: Conducting rigorous regression to the points along the flowline of the pipe.
- Method 2: Picking two representative points at the start and end of each section to compute the slope gradient.

Method 2 can be used directly in the field in several apps, whereas method 1 requires additional office

processing. (Although in the future, integrating a workflow into an app to enable a more rigorous slope computation in the field would be feasible.) Next, the team compared the slopes for each section computed with each method (table 3). The slopes differed by -0.46 percent on average. In all cases, the slopes estimated from PL were smaller than those obtained from the RTC360. Interestingly, the R^2 values computed with the regression trendline from PL tended to be higher than those with the RTC360, likely because PL performed substantial smoothing and downsampling to the data, which resulted in loss of the finer scale fluctuations and deviations in the pipe surface that were captured in the RTC360 data. Those fluctuations result in a reduction in the R^2 value in the regression.

Figure 8. Graph. Comparison of the PL and RTC360 reference data in a vertical profile along the flow line.



Source: FHWA. Created using data from 3D Scanner App.^(2,3)

Table 3. Slope comparison between the PL and the RTC360 reference data.

Section (figure 8)	PL Slope (Regression) (percent)	PL (R^2)	PL Slope (two point)	RTC Slope (Regression) (percent)	RTC (R^2)	PL Slope (two point) (percent)	Slope Diff. (Regression) (percent)	Slope Diff. (two point) (percent)
1	-5.70	0.9903	-6.12	-5.38	0.9810	-5.87	-0.32	-0.24
2	-2.45	0.9685	-2.51	-1.94	0.9515	-2.11	-0.51	-0.40
3	-9.36	0.9996	-9.45	-9.35	0.9997	-9.20	-0.01	-0.25
4	-7.62	0.9923	-8.02	-6.95	0.9850	-7.50	-0.67	-0.52
5	-7.91	0.9964	-7.45	-7.13	0.9958	-6.77	-0.78	-0.68

Diff. = difference.

Tanner Creek

The Tanner Creek culvert is a 50-inch diameter, corrugated metal pipe with a constricted area due to debris. The culvert also has experienced substantial damage and distortion. Figure 9 shows an example of the data-collection process with one person operating the PL to scan the culvert and a second person following with a light source to help improve the data quality. The entire culvert length was scanned in a matter of minutes with PL (figure 10). Overall, the PL scans tended to be smoother than the RTC360 scans (figure 11).

The analysis of the data collected at this site focused on evaluating the capability of PL to capture the deformed shape and the obstructed area of the culvert (figure 10). The research team obtained 20 0.05-m thick, vertical cross sections for both PL and RTC360 reference scan data at coincident locations in CloudCompare.⁽⁹⁾

Figure 9. Photo. Example of PL data-collection process in the culvert.



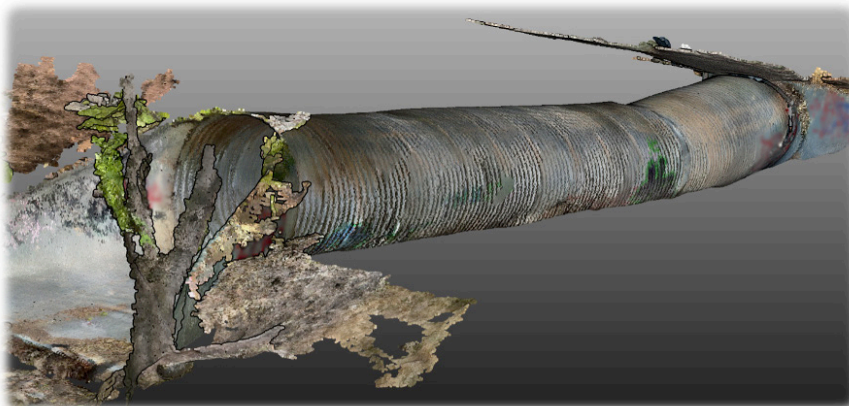
Source: FHWA.

Figure 10. Screenshots. Examples of the PL point clouds collected at Tanner Park.

A. View looking into pipe showing the substantial presence of debris and deviations from the circular shape.

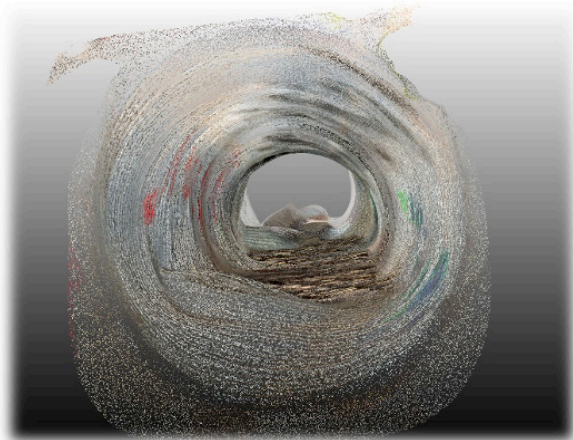


B. Side view of the pipe showing bending and other damages.



Source: FHWA. Created using data from 3D Scanner App visualized in CloudCompare version 2.13.^(2,3)

Figure 11. Screenshots. Example views of pipe showing the differences between PL and RTC360 reference scans.



Source: FHWA. Created using data from 3D Scanner App visualized in CloudCompare version 2.13.^(2,3)

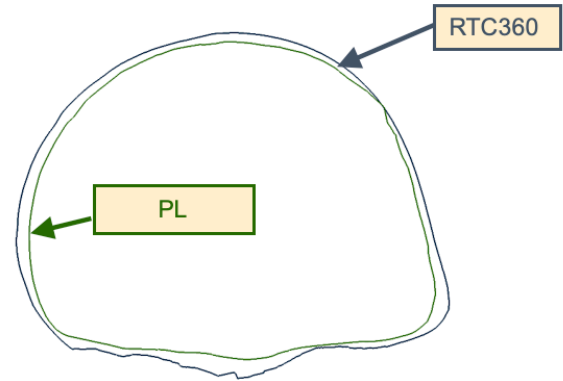
A. PL.



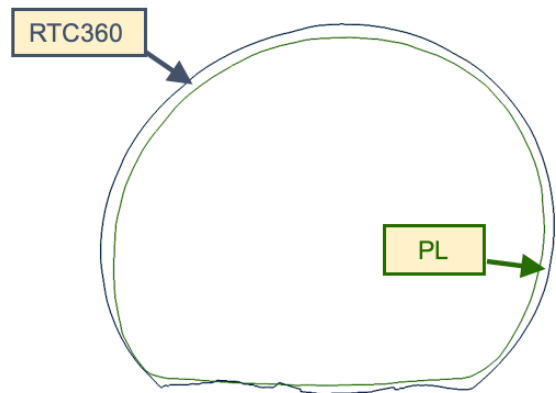
Source: FHWA. Created using data from RTC360 visualized in CloudCompare version 2.13.^(2,3)

B. RTC360.

Figure 12. Illustration. Example cross sections showing the shape differences between PL (inside) and RTC360 reference scans (outside).



A. Section 4.



B. Section 13.

Source: FHWA. Created using data from RTC360 and 3D Scanner App visualized in CloudCompare version 2.13.^(2,3)

Table 4. Comparison of pipe cross-sectional area between PL and the RTC360 reference scans: Nominal area = 1.17 m².

Statistic	Difference (m ²)	Percent Difference
Average	-0.084	-7.1
Std. dev.	0.038	3.2
Minimum	-0.136	-11.5
Maximum	-0.023	-1.9
RMS	0.092	7.8

For each cross section, a polygon was fitted to the data (figure 12) using CloudCompare's fitting tool. The area of each polygon was then computed based on a 2D reference plane of the polygon (table 4).

PL was able to capture the major deviations and distortion in the pipe; however, finer details such as the roughness and angularity of the debris, were smoothed in the PL data (figure 11 and figure 12). Nevertheless, the cross-sectional area of the pipe was comparable to the RTC360 reference data, with an RMS difference of 0.092 m² or 7.8 percent. As evidenced by the average difference of -0.084 m², PL tended to underestimate the cross-sectional area, likely because of the smoothing of the data on the corrugated surface of the pipe.

Hidden Grove

The research team captured the Hidden Grove culvert with a single pass from the outlet to the inlet with PL (figure 13) as well as with 14 scans with the RTC360 for reference. Given the steep slopes adjacent to the creek at the inlet, a closed loop survey was not possible. However, because the inlet and outlet were both in range of the scanner from the center of the culvert, drift would be minimal in the RTC360 data. The culvert had approximately 0.5 m of water inside that flowed at a very slow rate. The bottom of the culvert was damaged at the outlet, so the scanning commenced at a safe location in the culvert. However, approximately 4.5 m of the pipe were missed at the end of the culvert in the PL data as a result.

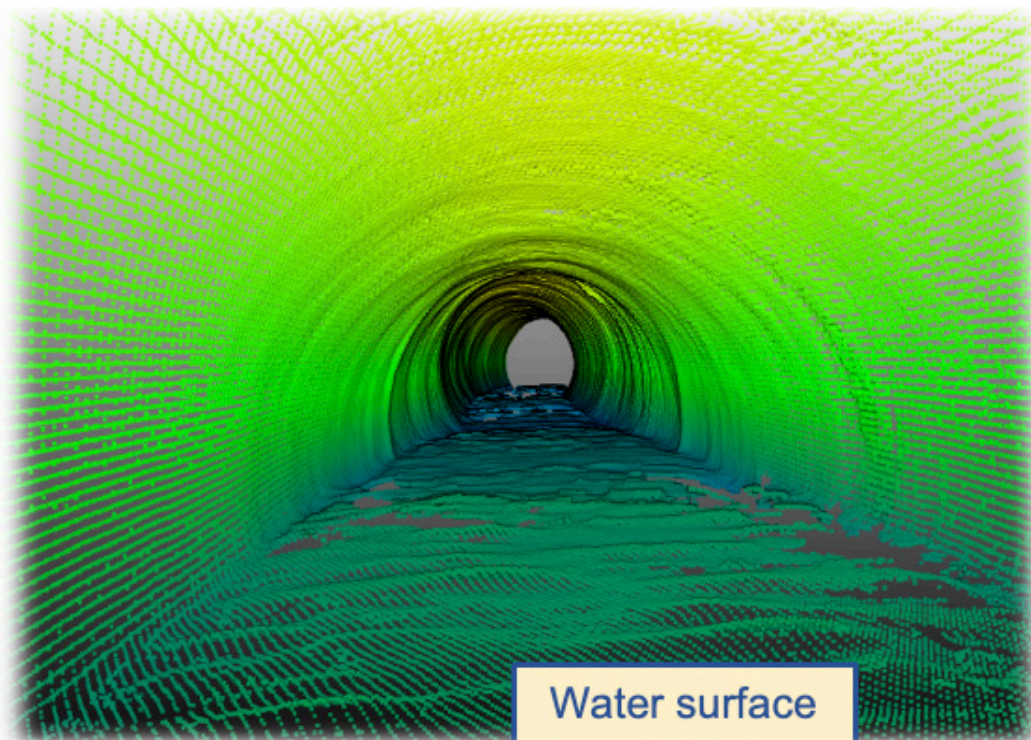
Given the length of the culvert and the relatively long scanning time of approximately 5 min to walk and scan the entire length, substantial subsampling occurred with this dataset. Generally good coverage of the culvert was obtained with few gaps. In figure 13, PL captured the water surface in the culvert; however, the surface was not reconstructed accurately because substantial ripple effects were observed in the surface that were not present in the field.

The team completed two versions of the analyses at this site to evaluate the impacts of the drift of the sensor

when scanning long segments (figure 14) (For more details on testing to evaluate the drift in PL for scanning long segments >10 m, refer to the FHWA report for this project.⁽¹³⁾):

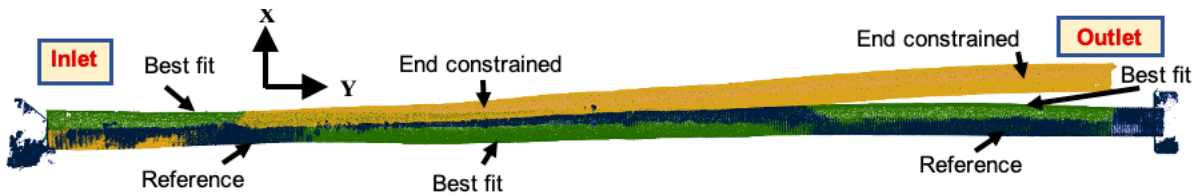
- In the first version, the PL point cloud was registered to the RTC360 data (translation X, Y, Z, and rotation Z) using the ICP algorithm in CloudCompare for the best overall fit.^(9,10) In this scenario, the ICP algorithm attempts to distribute the drift errors, which tends to result in the best matching in the middle of the scan and higher errors near the start and end of the scans. This scenario represents the ideal case when reference data are available to match the PL dataset in postprocessing.
- In the second version, a 15-m section of the PL scan at the inlet was used in the registration to the RTC360 reference data. This scenario is more representative of the drift error that would be observed in the field when operating PL from an initial starting point and progressing away from that point. In fact, in the field the PL scan commenced at the outlet. However, the outlet could not be fully scanned with PL due to safety issues from the damaged overhanging pipe. The inlet provided a clearer, consistent starting point for the evaluation.

Figure 13. Illustration. Example PL scan obtained in the Hidden Grove culvert.



Source: FHWA. Created using data from Scaniverse visualized in CloudCompare version 2.13.^(2,4)

Figure 14. Illustration. Drift observed in the PL scans using the best fit and end-constrained registration approaches compared to the RTC360 reference data.



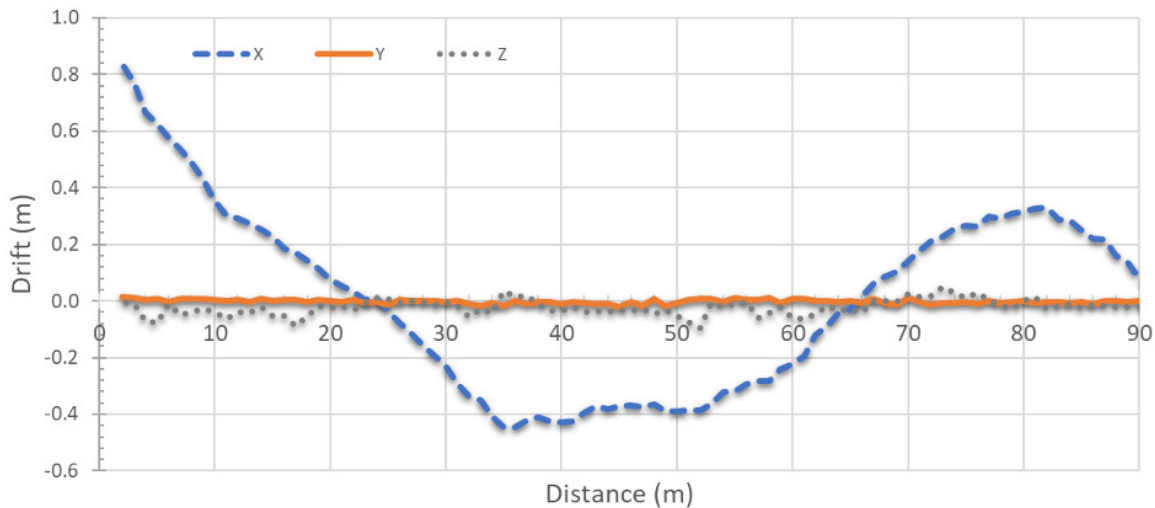
Source: FHWA. Created using data from RTC360 and Scaniverse visualized in CloudCompare version 2.13.^(2,4)

For simplicity of interpretation, the data were rotated about the Z-axis such that the Y direction is aligned with the flow direction of the pipe to determine the circle centers for the cross sections. The X direction represents the transverse offsets associated with the drift. The Z direction was not transformed in this rotation. The Z direction represents the tilting errors and any vertical drift associated with PL.

Figure 15 presents the drift results from the first method of the best overall fit. Figure 16 contains the drift results from the second method of constraining to the initial portion of the pipe at the inlet. Table 5 provides a comparison of the statistics between the two methods.

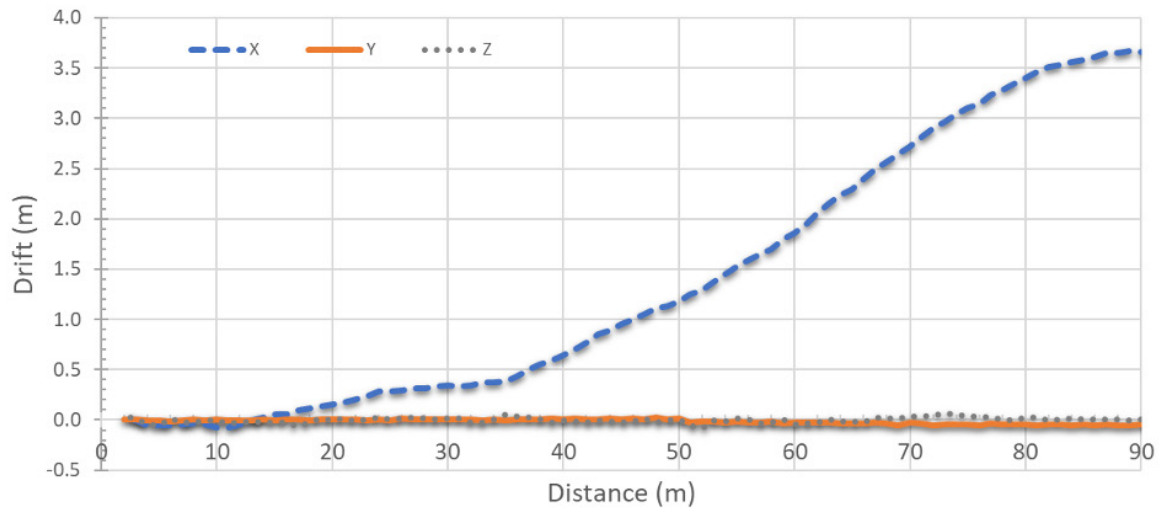
Low drift values are observed in the Y direction under both scenarios given that the cross sections were taken along the Y axis. Slight deviations occur in the cross-sectional width of 0.05 m. Nevertheless, given that the pipe corrugation is several centimeters in size, this slight deviation can result in some differences in the circles' fit to the cross section and the dimensions extracted. Some errors in the Z direction are notable in the results as well. For the best overall fit registration, drift still exists in the data; however, that drift is balanced more across the dataset compared with the end-constrained method where error is allowed to continue to propagate with distance from the initial starting point.

Figure 15. Chart. X, Y, and Z deviations and drift of PL compared to the reference data with the best overall fit registration.



Source: FHWA.

Figure 16. Chart. X, Y, and Z deviations and drift of PL compared to the reference data with the end-constrained registration.



Source: FHWA.

Table 5. Comparison of circle fit centers of PL compared with RTC360 for the Hidden Grove culvert between the best overall fit and end-constrained registration for 90 cross sections.

Statistic	Best Overall Fit			End Constrained		
	ΔX	ΔY	ΔZ	ΔX	ΔY	ΔZ
Average (m)	0.006	-0.002	-0.022	1.410	-0.016	-0.001
Std. dev. (m)	0.324	0.007	0.028	1.316	0.023	0.027
Minimum (m)	-0.447	-0.019	-0.094	-0.077	-0.058	-0.087
Maximum (m)	0.835	0.014	0.049	3.675	0.026	0.065
RMS (m)	0.322	0.008	0.035	1.924	0.028	0.026
95 percent conf. (m)	0.632	0.015	0.070	3.771	0.054	0.052

Table 6 provides the circle-fitting results of RMS, radius, and slope compared with the RTC360 reference data for the Hidden Grove Culvert, similar to the analysis completed for Lisa Falls. Notably, the RMS fitting values are substantially higher (0.020 m RMS versus 0.014 m), and more deviations are observed in the radius (0.019 m RMS versus 0.010 m RMS) given the increased difficulty of fitting a circle to a cross section of a corrugated pipe as a result of the variability of the radius throughout the pipe. Similarly, the estimated

slope values are substantially higher compared with Lisa Falls given the fluctuations with the corrugations of a few centimeters, affecting the elevation values of the minimum point on the circle fits and the fact that the bottom of the pipe was not visible. Because the cross sections were extracted at 1-m increments, even small deviations in elevation can have a substantial affect in slope calculations. Table 7 provides the results from the end-constrained registration, which are very similar to the best overall fit registration.

Table 6. Circular fitting results of the PL compared with the PL for the Hidden Grove Culvert with best overall fit registration for 90 cross sections.

Statistic	RMS (PL)	RMS (RTC360)	Δ RMS	Δ Radius	Δ Slope (percent)
Average (m)	0.019	0.017	0.002	-0.005	-0.12
Std. dev. (m)	0.007	0.006	0.008	0.019	0.42
Minimum (m)	0.008	0.008	-0.012	-0.047	-0.74
Maximum (m)	0.047	0.049	0.034	0.039	0.79
RMS (m)	0.020	0.019	0.008	0.019	0.43
95 percent conf. (m)	0.039	0.036	0.016	0.038	0.84

Table 7. Circular fitting results of PL compared with PL for the Hidden Grove Culvert with best overall fit registration for 90 cross sections.

Statistic	RMS (PL)	RMS (RTC360)	Δ RMS	Δ Radius	Δ Slope (percent)
Average (m)	0.019	0.017	0.002	-0.004	-0.03
Std. dev. (m)	0.007	0.006	0.008	0.019	4.15
Minimum (m)	0.009	0.008	-0.013	-0.052	-11.90
Maximum (m)	0.040	0.049	0.030	0.038	8.72
RMS (m)	0.020	0.019	0.008	0.019	4.13
95 percent conf. (m)	0.039	0.036	0.015	0.038	8.10

Parley's Creek

The research team captured the entire culvert located near Parley's Creek Pavilion at Sugar House Park with PL (figure 17). Some RTC360 reference data were obtained on the exterior and for a small portion of the pipe on the inlet side; however, the water levels and flow rates were too high to safely operate the RTC360 scanner inside the culvert, especially given a hydraulic jump present in the culvert. Nevertheless, PL could safely be operated for the entire length. Here, the team

used PL to capture details on a clogged catch basin (figure 18). These details could not be distinguished in the point cloud data but were adequately captured in the texture map of the mesh. In comparison to an ordinary photograph, which provides excellent texture information, the point cloud data offer a more precise location of the feature with respect to the entire culvert. In addition, the 3D representation of the surrounding environment helps put those features in context.

Figure 17. Screenshot. Example scan of the entrance of the Parley's Creek pavilion culvert.



Source: FHWA. Created using data from 3D Scanner App visualized in CloudCompare version 2.13.^(2,3)



A. Clogged catch basin near the inlet.



B. Unclogged catch basin near the outlet.

Source: FHWA. Created using data from 3D Scanner App visualized in CloudCompare version 2.13.^(2,3)

KEY FINDINGS AND FUTURE OPPORTUNITIES

The research team learned the following lessons during the process of scanning the culverts with PL:

- PL's fast processing rate (a few minutes) was helpful in investigating the quality of the scan data and identifying missing gaps to determine if any additional data collection was necessary.
- An external, handheld light source was required to scan most of the culverts because of the poor lighting conditions inside. (An external, handheld light source was also important for safety reasons.) However, for culverts 10-m long or shorter, the lighting conditions were generally adequate to capture data without the light source. The headlamps or smaller attachment lights did not provide sufficient ambient lighting for quality data capture with PL. Further, these lights tended to concentrate the light in a small area compared with the field of view of PL.
- Having at least two people in the field crew was important. One person operated PL and the second person operated a light source and pointed out safety concerns.
- The team was able to capture culverts as small as 48 inches in diameter given mobility constraints for the operator in the pipe. Water or debris may also limit mobility in these smaller culverts. If the pipe is free of debris, a small diameter could be scanned by using a roller. Creating a robotic platform with a pivot and the PL attached, allowing PL to rotate, would be another possibility. However, these methods were beyond the scope of this case study.
- Large culverts (e.g., Midas Creek) were challenging to capture due to the range limitations of the scanner. Multiple passes at different sections of the culvert can mitigate this limitation. However, such an approach requires additional postprocessing and could potentially lead to gaps in the data capture because results could not be investigated in the field.
- Scans needed to be performed at low flow rates where the culverts could be navigated safely. Several sites had flows too high for a static scanner but could be captured with PL.
- PL obtained measurements of length (a few cm RMS), radius (<1 cm RMS), slopes (0.5 percent), and area (within 8 percent RMS) that were generally consistent with the RTC360 reference data for smooth RCP and PVC pipes. These measurements proved more challenging for corrugated pipes because of the fluctuations in the surface.

- Substantial lateral drifting occurred in PL data for culvert sections beyond 10 m in length. Relative measurements, such as the area and radius or the length measurements, were not substantially affected; however, this drifting affected integration with other datasets and would likely affect analyses with the data.
- PL's Global Navigation Satellite System (GNSS) capabilities allowed the scan to be georeferenced for integration with asset management databases. However, GNSS did not work inside the culvert.

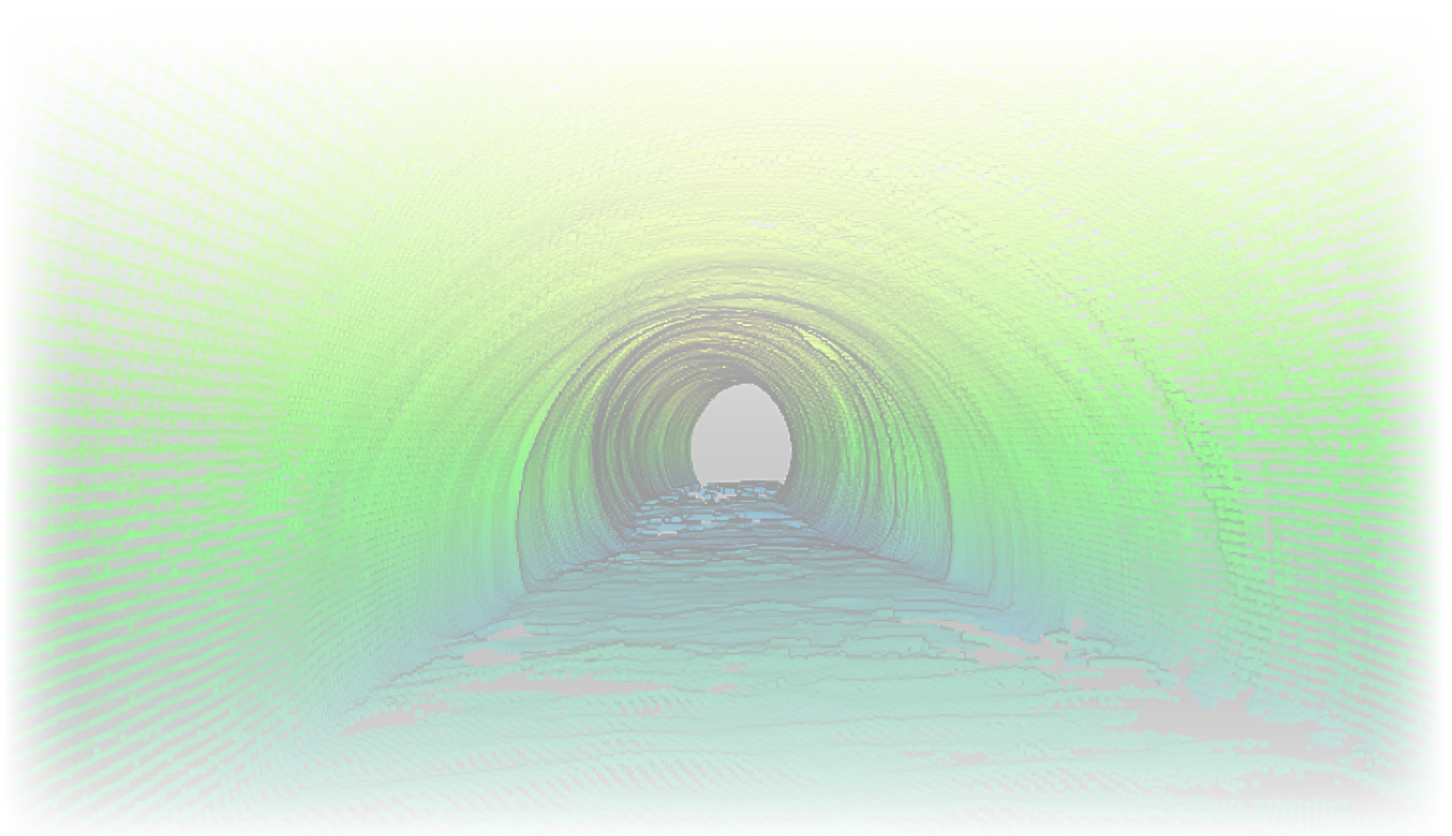
ACKNOWLEDGEMENTS

The Natural Hazards Engineering Research Infrastructure Rapid Response Research Facility funded by the U.S. National Science Foundation under grant CMMI-2130997 provided equipment and software used in this study. Abdul Wakil from UDOT provided assistance with this case study and the demonstrations.

REFERENCES

1. Schall, J. D., P. L. Thompson, S. M. Zerges, R. T. Kilgore, and J. L. Morris. 2012. *Hydraulic Design of Highway Culverts Third Edition—Hydraulic Design Series Number 5*. Report No. FHWA-HIF-12-026. Washington, DC: Federal Highway Administration.
2. CloudCompare. n.d. "CloudCompare (GPL)" (GPL software and configuration files in GitHub repository). Version 2.13. <https://github.com/cloudcompare>, last accessed October 25, 2024.
3. Laan Labs. 2024. *3D Scanner App* (software). <https://3dscannerapp.com/>, last accessed October 25, 2024.
4. Niantic, Inc. 2024. *Scaniverse* (software). <https://scaniverse.com/>, last accessed October 25, 2024.
5. Abound Labs Inc. 2024. *Metascan* (software). <https://metascan.ai/>, last accessed October 25, 2024.
6. Pix4D SA. 2024. *PIX4D* (software). <https://www.pix4d.com/>, last accessed October 30, 2024.
7. Leica Geosystems. 2023. *Cyclone CORE* (software). <https://leica-geosystems.com/en-us/products/laser-scanners/software>, last accessed December 27, 2023.
8. EZDataMD, LLC. 2023. *EZVox* (software). <https://ezdatamd.com/products/>, last accessed December 18, 2023.
9. Che, E., and M. J. Olsen. 2023. "Vo-Norvana: Versatile Framework for Efficient Segmentation of Large Point Cloud Data Sets." *Journal of Computing in Civil Engineering* 37, no. 4: 04023012.

10. Bai, H. 2022. *ICP Algorithm: Theory, Practice and Its SLAM-oriented Taxonomy*. Champaign, IL: University of Illinois Urbana-Champaign. <https://arxiv.org/pdf/2206.06435>, last accessed October 22, 2024.
11. EZDataMD, LLC. 2023. *EZFitter* (software). <https://ezdatamd.com/products/>, last accessed December 18, 2023.
12. Olsen, M. J., E. Johnstone, F. Kuester, S. A. Ashford, and N. Driscoll. 2011. “New Automated Point-Cloud Alignment for Ground Based Lidar Data of Long Coastal Sections” *Journal of Surveying Engineering* 137, no. 1: 14–25. [http://dx.doi.org/10.1061/\(ASCE\)SU.1943-5428.0000030](http://dx.doi.org/10.1061/(ASCE)SU.1943-5428.0000030), last accessed October 25, 2024.
13. Olsen, M. J., E. Che, J. Jung, M. Thorsen, J. Caya, and G. Roe. (Forthcoming.) *Leveraging Pocket Lidar for Construction Inspection and Digital As-Builts—Phase I*. Washington, DC: FHWA.



Source: FHWA. Created using data from Scaniverse visualized in CloudCompare version 2.13.^(2,4)

Researchers—This study was conducted by EZDataMD, LLC; 5C Strategy; and MPN Components, Inc. in collaboration with Utah LTAP and UDOT. Michael Olsen (EZDataMD, LLC), John Caya (5C Strategy), and Gene Roe (MPN Components, Inc.) were researchers under order number 693JJ321P000047. Randy Wahlen and Joseph Perrin (Utah LTAP) and Aaron Mackliet (Utah State University) contributed to this case study.

Distribution—This TechNote is being distributed according to a standard distribution. Direct distribution is being made to the FHWA divisions and Resource Center.

Availability—This TechNote may be obtained at <https://highways.dot.gov/research>.

Key Words—Pocket lidar, culverts, measurements, slope, pipes.

Notice—This document is disseminated under the sponsorship of the U.S. Department of Transportation (USDOT) in the interest of information exchange. The U.S. Government assumes no liability for the use of the information contained in this document.

Non-Binding Contents—Except for the statutes and regulations cited, the contents of this document do not have the force and effect of law and are not meant to bind the States or the public in any way. This document is intended only to provide information regarding existing requirements under the law or agency policies.

Quality Assurance Statement—The Federal Highway Administration (FHWA) provides high-quality information to serve Government, industry, and the public in a manner that promotes public understanding. Standards and policies are used to ensure and maximize the quality, objectivity, utility, and integrity of its information. FHWA periodically reviews quality issues and adjusts its programs and processes to ensure continuous quality improvement.

Disclaimer for Product Names and Manufacturers—The U.S. Government does not endorse products or manufacturers. Trademarks or manufacturers' names appear in this document only because they are considered essential to the objective of the document. They are included for informational purposes only and are not intended to reflect a preference, approval, or endorsement of any one product or entity.